Quaternary Research (2023), **112**, 36–50
doi:10.1017/qua.2022.44

Research Article

Implications of the loess record for Holocene climate and human settlement in Heye Catchment, Jiuzhaigou, eastern Tibetan Plateau, Sichuan, China

Amanda H. Schmidt[a]*, Brian D. Collins[b], Amanda Keen-Zebert[c], Jade d'Alpoim Guedes[d], Anke Hein[e], Andrew Womack[f], Casey McGuire[a], James Feathers[g], Lyman Persico[h], Dominic Fiallo[a], Ya Tang[i] and Bruce Simonson[a]

[a]Department of Geosciences, Oberlin College, Oberlin, Ohio 44074, USA; [b]Department of Earth and Space Sciences, University of Washington, Seattle, Washington 98195, USA; [c]Division of Earth and Ecosystem Sciences, Desert Research Institute, 2215 Raggio Parkway, Reno, Nevada 89512, USA; [d]Scripps Institution of Oceanography, Department of Anthropology, University of California San Diego, La Jolla, California 92034, USA; [e]School of Archaeology, University of Oxford, Oxford OX1 3TG, UK; [f]Department of Asian Studies, Furman University, 3300 Poinsett Highway, Greenville, South Carolina 29613, USA; [g]Department of Anthropology, University of Washington, Seattle, Washington 98195, USA; [h]Geology and Environmental Science, Whitman College, Walla Walla, Washington 99362, USA and [i]Department of Environment, College of Architecture and Environment, Sichuan University, Chengdu, Sichuan 610065, China

Abstract

We examine the Holocene loess record in the Heye Catchment on the margins of the Tibetan Plateau (TP) and China Loess Plateau (CLP) to determine: the region to which the Heye Catchment climate is more similar; temporal change in wind strength; and modification of the loess record by mass wasting and human activity. Luminescence and radiocarbon dating demonstrate loess deposited in two periods: >11–8.6 ka and <5.1 ka. The 8.6–5.1 ka depositional hiatus, which coincides with the Mid-Holocene Climatic Optimum, is more similar to the loess deposition cessation in the TP than to the loess deposition deceleration in the CLP. Grain-size analysis suggests the Heye loess is a mixture of at least three different grain-size distributions and that it may derive from multiple sources. A greater proportion of coarse sediments in the older loess may indicate stronger winds compared with the more recent depositional period. Gravel incorporated into younger loess most likely comes from bedrock exposed in slump scarps. Human occupation of the catchment, for which the earliest evidence is 3.4 ka, postdates the onset of slumping; thus the slumps may have created a livable environment for humans.

Keywords: Loess, Landslides, Tibetan Plateau, Archaeology, Mid-Holocene Climatic Optimum, Jiuzhaigou

(Received 7 April 2022; accepted 28 July 2022)

INTRODUCTION

Situated on the margins of both the Tibetan Plateau (TP) and the China Loess Plateau (CLP), Holocene loess deposits in Jiuzhaigou, northern Sichuan (Fig. 1), provide an opportunity to add to the understanding of the spatial variation in Holocene climate and loess provenance in western China. In addition, the region's oldest archaeological site (d'Alpoim Guedes et al., 2015) is in Jiuzhaigou loess deposits on hillslopes subject to landsliding and co-seismic faulting. Previous investigations of loess in Jiuzhaigou (Wen et al., 2014, 2017) left unanswered questions about the depositional history and provenance of the loess and also the role of hillslope processes and seismic activity in modifying the loess and hillslope topography. Thus, in addition to enhancing understanding of Holocene climate and loess provenance in western China, analysis of the Jiuzhaigou loess record can also provide insight into causal connections between climate, loess deposition, hillslope deformation by landslides and co-seismic faulting, and human inhabitance.

Analysis of the age of loess and loess–paleosol sequences in the CLP and TP has been widely used to examine regional paleoclimate (e.g., Derbyshire, 1982; An et al., 1991; Lehmkuhl et al., 2000, 2014; Porter, 2001; Lehmkuhl and Owen, 2005; Sun et al., 2007; Pullen et al., 2011; Stauch et al., 2012), because loess generally deposits during cool and dry periods, whereas paleosols generally form on loess deposits during intervening wet and warm periods (Porter, 2001). The grain size of loess may also provide information on wind speed (e.g., An et al., 1991; Xiao et al., 1995; Jiang and Ding, 2010), aridity and frequency of storms (An et al., 1991), loess sources and paleowind directions (Sun et al., 2004; Prins et al., 2009; Yang et al., 2010a), and the relative importance of low-altitude and high-altitude eolian transport of loess (Sun et al., 2004; Nottebaum et al., 2015). While loess–paleosol sequences up to 400 m thick in the CLP provide valuable paleoclimate data for at least the last 2.4 Ma (Porter, 2001), there has been less study of either Holocene loess in China (Maher et al., 2003; Kuster et al., 2006) or loess in China outside the CLP (Yang et al., 2010a, 2010b; Lehmkuhl et al., 2014).

*Corresponding author at: Department of Geosciences, Oberlin College, Oberlin, Ohio 44074. E-mail address: aschmidt@oberlin.edu (A.H. Schmidt).

Cite this article: Schmidt AH *et al* (2023). Implications of the loess record for Holocene climate and human settlement in Heye Catchment, Jiuzhaigou, eastern Tibetan Plateau, Sichuan, China. *Quaternary Research* **112**, 36–50. https://doi.org/10.1017/qua.2022.44

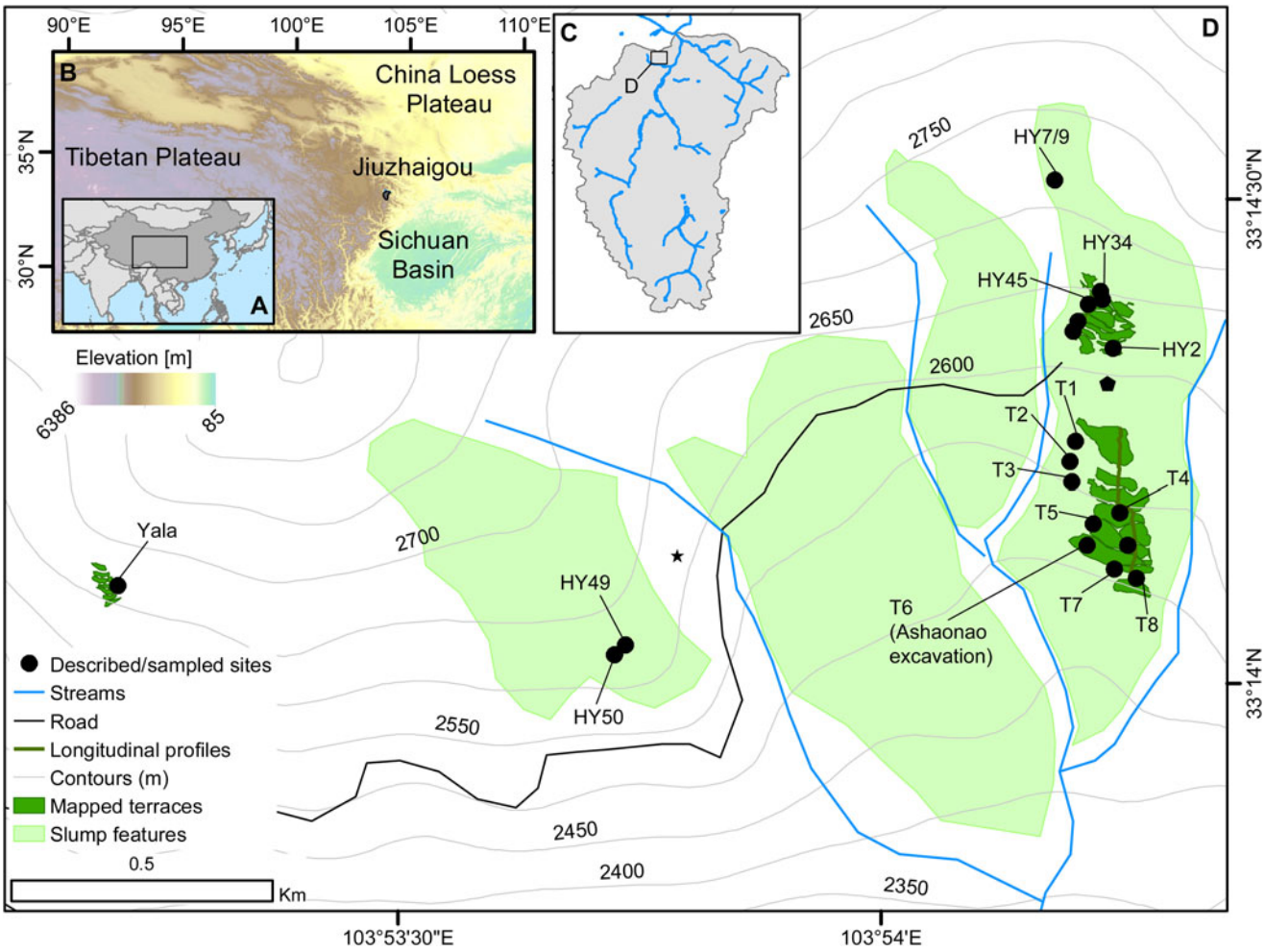

Figure 1. Context map showing (A) location of study area in Asia with area of B outlined; (B) location of Jiuzhaigou and approximate boundaries of other loess regions in China with topography; (C) location of Heye within Jiuzhaigou; and (D) location of study site with specific terraces, longitudinal profiles, approximate boundaries of slump features identified in the field, location of Fig. 3A (marked with a star), and other important features identified. Contours are derived from GDEM data (LP DAAC, 2001).

In western China, Holocene loess deposits and their associated soils, which span the TP, western Xinjiang Province, the CLP, and south to the Sichuan basin, and climate proxies from cave formations and lake and bog cores generally record a cool and dry climate in the Early and Late Holocene, with an intervening warmer and wetter period during the Mid-Holocene Climatic Optimum (MHCO; Maher et al., 2003; Kuster et al., 2006; Nottebaum et al., 2015), but the loess record also shows within-region variation in the depositional response to climate (An et al., 2000). For example, in the CLP, loess deposited continuously in both cool, dry periods and warm, wet periods, but deposition slowed and soil formation increased during wetter and warmer conditions (Huang et al., 2003). In other locations, loess accumulated sporadically: in some places, loess accumulated only during cool and dry periods, while in other places, loess accumulated in wet and warm periods, when increased vegetation enhanced the efficacy of dust trapping, with a hiatus in deposition during cool and dry periods (Lehmkuhl et al., 2000, 2014; Kuster et al., 2006; Sun et al., 2007).

Loess tends to become finer the farther it travels, and thus fines downwind (Liu and Ding, 1998; Nugteren and Vandenberghe, 2004; Yang et al., 2010a). West-to-east fining of loess on the CLP (An et al., 1991; Porter, 2001) implies a source from the west; various studies suggest a source or mix of sources in the northern TP, the Qaidam basin, the Gobi Desert, and/or the Taklamakan Desert (Derbyshire et al., 1998; Sun et al., 2000; Maher et al., 2009; Stevens et al., 2010; Wu et al., 2010; Pullen et al., 2011), and some argue that loess sources are different during glacial and interglacial times, with deserts dominating during interglacial periods and the TP and Qaidam basin dominating during glacial periods (Pullen et al., 2011; Fig. 2). Similarly, downwind fining has been used to determine that the loess in the Sichuan basin of northern Sichuan comes from the eastern TP rather than the CLP (Yang et al., 2010a; Wen et al., 2014). Jiuzhaigou is located on the margins of the CLP, TP, and Sichuan basin, and prior studies suggest that the loess is sourced from the eastern TP (e.g., Wen et al., 2014). However, it is unknown if loess source or wind speed changed during the period of loess deposition.

As early as 1977, scientists identified three dominant modes of airborne dust and interpreted these modes as having different transportation mechanisms and source materials (Patterson and Gillette, 1977). Although descriptive statistics such as mean, standard deviation, and skewness (Folk, 1980) can be calculated for

https://doi.org/10.1017/qua.2022.44 Published online by Cambridge University Press

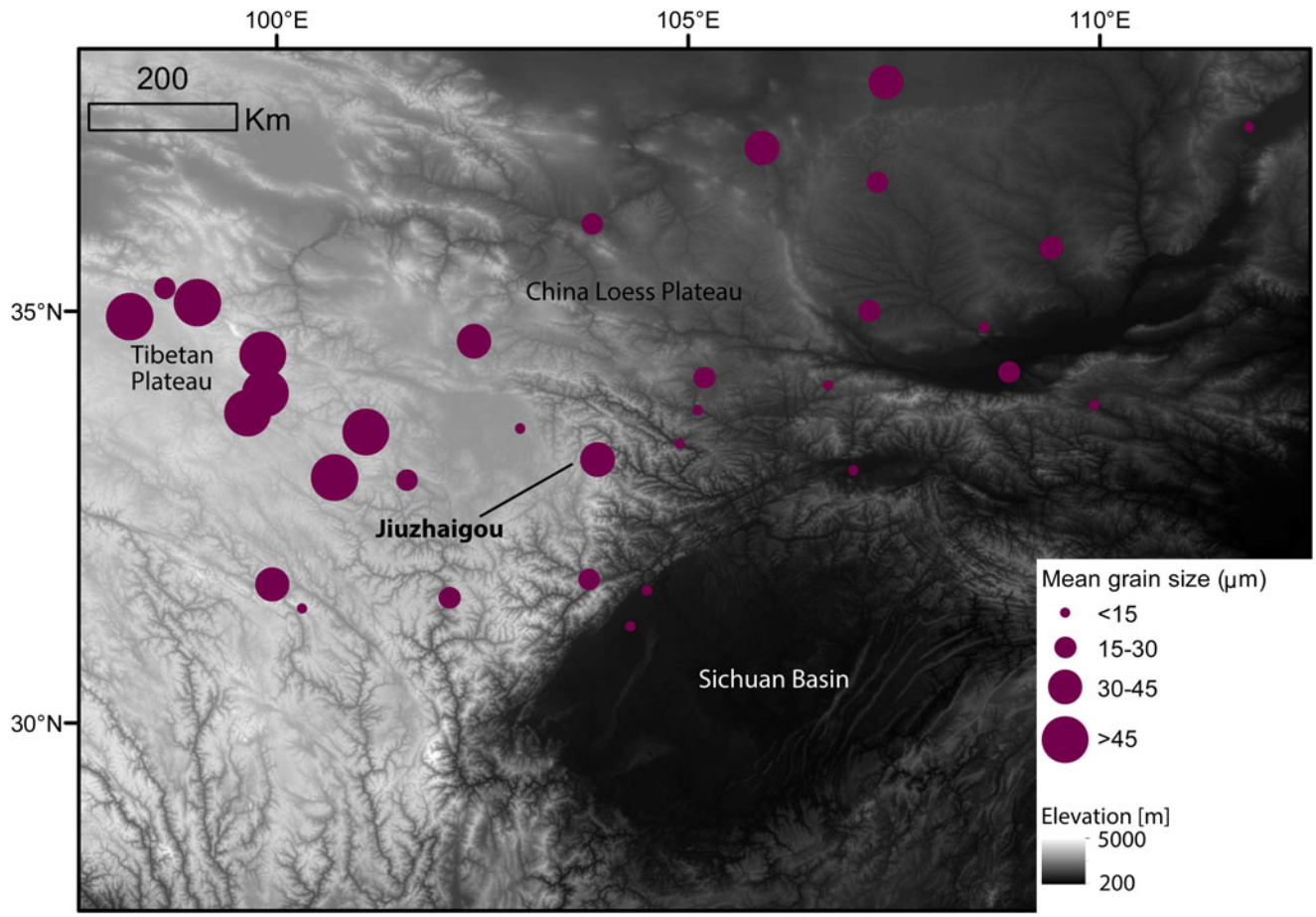

Figure 2. Distribution of grain-size data from Jiuzhaigou (marked on map with bold name; data from Wen et al. [2014]) and previous studies on loess grain size in the region (Lei, 1998; Wang et al., 2003; Sheng, 2010; Yang et al., 2010a; Stauch et al., 2012; Lehmkuhl et al., 2014); size of point indicates reported mean grain size. Background elevation is from World Wildlife Fund (2008).

multimodal samples, these statistical metrics are not particularly meaningful for mixed materials (Dietze et al., 2012). Prior work determining components of mixed grain-size samples relies on end-member modeling analysis (e.g., Dietze et al., 2012) or single-specimen unmixing (Sun et al., 2004; Qin et al., 2005; Xiao et al., 2009, 2013; Pye, 2015), typically using either Weibull (Sun et al., 2004) or lognormal (Qin et al., 2005; Xiao et al., 2009; Pye, 2015) distributions in the modeling. For multimodal samples, different peaks are attributed to different dust sources (Vandenberghe, 2013). Most studies identify at least two fractions: a coarser fraction interpreted to be from the local area and transported up to a few kilometers during dust storms and a finer fraction interpreted to be non–dust storm dust sourced from locations more than a few kilometers away (Patterson and Gillette, 1977; Sun et al., 2004; Vandenberghe, 2013; Pye, 2015). Some studies identify multiple intermediate modes that are interpreted as either a mixture of other modes or additional transport distances (Vandenberghe, 2013). Occasionally submicron-sized dust is observed, and this is interpreted as either anthropogenic particles, weathering materials, or long-range transported dust (Patterson and Gillette, 1977; Zhang et al., 1994). CLP loess has two modes that are interpreted as non–dust storm dust transported long distances on the high westerly winds and more locally sourced material that is coarser and transported during dust storms (Sun et al., 1998, 2004). The northeastern TP loess has two to three modes that are fine sandy, coarse silt, and medium silt in size (Vriend and Prins, 2005; Nottebaum et al., 2015), and the ratio of the medium silt to coarse silt modes may indicate the relative strength of local winds as opposed to high westerlies transporting finer particle sizes (Nottebaum et al., 2014). The grain size of loess in Jiuzhaigou has not been analyzed in this way, and thus the potential for different contributions from different locations beyond the eastern TP source area previously identified (Wen et al., 2014) has not been explored, possibly because accessible software to do these calculations only recently became available (Liu et al., 2021).

The loess record can also contribute to an understanding of the Holocene history of human inhabitance of western China. For example, the timing of loess deposition, and implied climatic fluctuations, can correspond to changes to human habitation in loess regions of western China (An et al., 2005; d'Alpoim Guedes et al., 2015; Wen et al., 2017), because agriculturalists can preferentially inhabit areas of loess soils (Henck et al., 2010; Schmidt et al., 2017). However, the widespread landslide hazards reported in loess regions (Dijkstra et al., 1994; Derbyshire, 2001; Wen et al., 2005; Zhang and Wang, 2007; Schmidt et al., 2017) also compromise safety (Schmidt et al., 2017). Conversely, human inhabitance can modify the loess record; for example, farming can inflate the rate of loess deposition (Roberts et al.,

https://doi.org/10.1017/qua.2022.44 Published online by Cambridge University Press

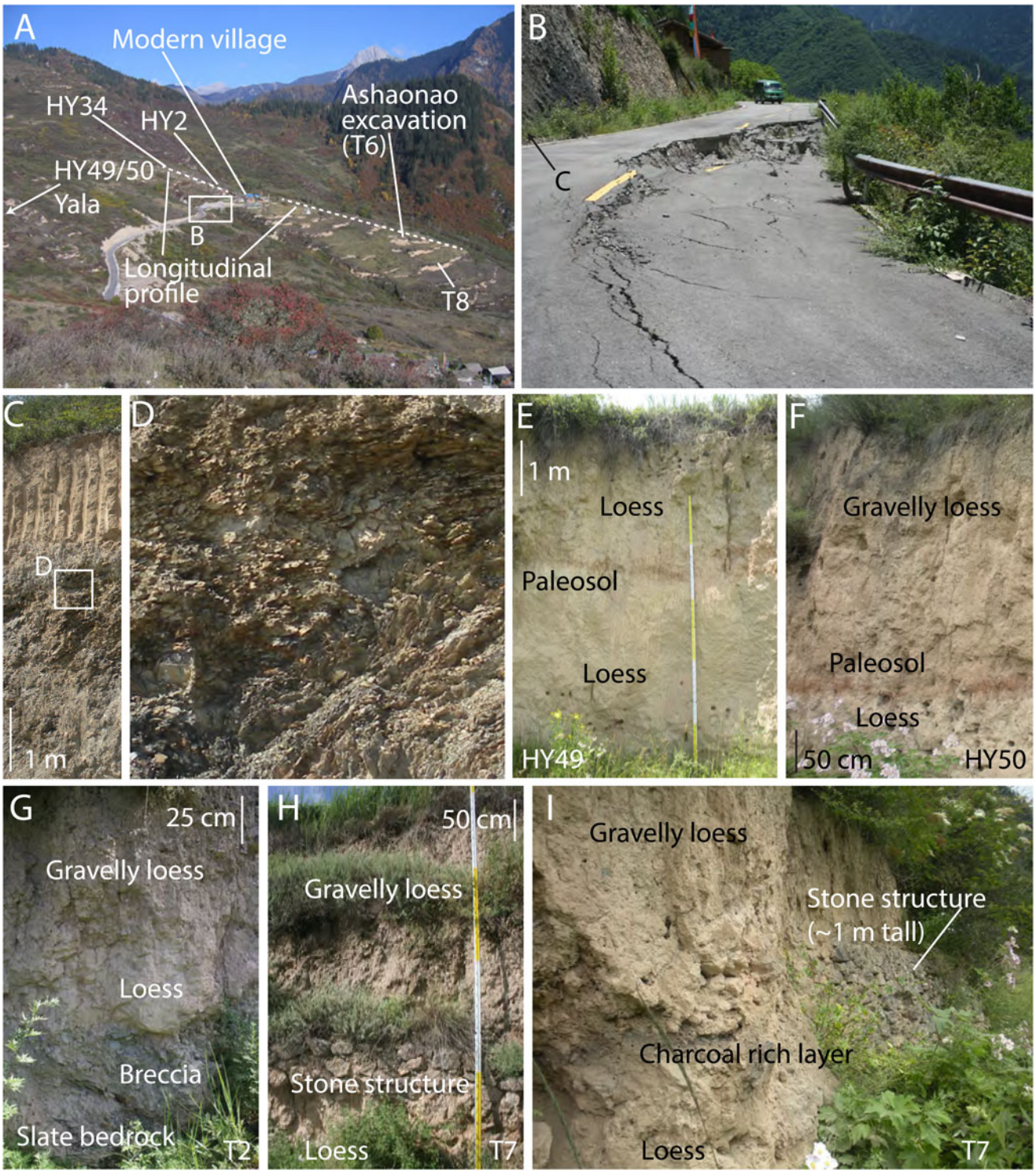

Figure 3. Photos of the study valley. (A) View looking north across Heye Catchment showing the series of slump block terraces (tens to hundreds of meters across, up to ~10 m tall). Location given on Fig. 1D with a star. Longitudinal profile line corresponds to transect in Fig. 5. (B) Close-up of the road to the upper parts of the valley. The road was completed in 2008 and was already unpassable in 2011. (C) Deformed bedrock topped by loess exposed in a road cut. (D) Zoom in of box in C showing deformed bedrock. (E) Loess–paleosol–loess sequence at HY49 (location shown in A). (F) Loess–paleosol–gravelly loess sequence that is typical of scarps in Heye Catchment. (G) Deformed bedrock, breccia, loess, and gravelly loess sequence from T2. (H) Loess, stone structure, and gravelly loess sequence shown from T7. (I) Stone structure and a charcoal-rich layer in addition to loess and gravelly loess (T7, to the left of photo in H). Scarp locations for E–I given in Figs. 1 and 6. Sketches of terrace risers are available in Supplementary Figs. S1–S10.

2001), farming is associated with soil loss in loess areas (Lowdermilk, 1924), and land uses could also potentially destabilize loess-mantled slopes (Lacroix et al., 2020).

Here we analyze the loess record in Heye Catchment, Jiuzhaigou, Sichuan, to add to the understanding of how loess deposition varies temporally within western China in response

https://doi.org/10.1017/qua.2022.44 Published online by Cambridge University Press

to regional Holocene climate; determine the provenance of loess deposited in the Jiuzhaigou area; understand the mechanisms through which the loess record may have been altered during or following deposition; and better understand Holocene relations between loess and human inhabitance in northwestern Sichuan Province.

STUDY SITE

Our study site is located in Heye Catchment, Jiuzhaigou National Nature Reserve (33°13′N, 103°55′E), a World Heritage Site in the Minshan Mountains (Fig. 1). Mean annual temperature is 6°C and mean annual precipitation is 650 mm, with the majority of precipitation falling during the summer monsoon (Qiao et al., 2016). The elevation of the Heye Catchment ranges from 2200 m at its outlet to the main Jiuzhaigou valley to 4000 m on the catchment's southern boundary.

The catchment is primarily formed in limestone and dolomite with lesser amounts of phyllite and slate and is locally mantled by up to 10 m of loess (Guo et al., 2006). The region is tectonically active and was subject to shaking from both the 2008 Wenchuan earthquake and the 2017 Jiuzhaigou earthquake (Sun et al., 2018). The Heye and Longkang Faults are near, or cross through, Heye Catchment, but contradictory locations on available, published maps and/or the small scale of those maps (Zhang and Xu, 1993; Guo et al., 2006; Burchfiel and Chen, 2012) leaves their precise locations uncertain. The timing of previous movement on the faults is unknown (Zhang and Xu, 1993). Spatially extensive slump earthflows on east-, south-, and west-facing loess-covered slopes are characterized by terraces with 1- to 10-m-tall risers (Figs. 1 and 2, Supplementary Figs. S1–S10). One of these slump features, on which most of our observations are concentrated, consists of a series of slump blocks having near-horizontal surfaces, or terrace treads, and near-vertical failure planes, or terrace risers; has an area of 10.5 hectares; is covered in loess up to 10 m thick; and may have been destabilized by the Heye Fault (Zhang and Xu, 1993).

Deformed phyllite and slate are exposed at the base of some of these terrace risers. The exposed bedrock is overlain by either the older of two distinct loess units or by the younger of the two loess units. A red horizon caps the older loess in most exposures. The older loess sometimes includes mollusks, but not charcoal. At one exposure (HY49), measured levels of soil carbon and nitrogen in the red layer are similar to levels in the modern soil, indicating the red layer is likely a paleosol (Henck et al., 2010). Because this stratigraphy is similar throughout the Heye Catchment, and the red layers have the same appearance as the paleosol at HY49, we interpret red layers elsewhere in the catchment to be paleosols. A paleosol is visible in most, but not all, terrace scarps.

A younger loess overlies the paleosol or in some locations directly overlies the exposed bedrock. The younger loess consists of a silty matrix supporting angular, lithic clasts ranging in size from 2 mm particles to 1 m blocks. The paleosol and gravelly loess in some exposures contain archaeological artifacts, usually charcoal, and do not contain mollusks. In one terrace riser exposure (HY49), the paleosol is topped by loess instead of gravelly loess; this is the only location where the paleosol is covered by loess without gravel. All terrace risers contain outcrops of younger loess (typically gravelly loess), and more than half (~60%) contain older loess.

Geologic hazards in Jiuzhaigou, and in Heye Catchment in particular, have been studied due to high levels of tourism and possible risk to visitors. Debris flows in the reserve, which reportedly have increased in frequency in recent years due to human activity (Zhang, 2019), are common. Slope stabilization structures for diverting flows away from tourist areas have been used to mitigate hazards, as in national parks elsewhere in China (Cui et al., 2003, 2007). In our study area, Heye Catchment, debris-flow hazard management has focused on dams and channels to divert flows away from the relatively large village near the mouth of the valley (Cui et al., 2003). In addition to debris flows, the slump earthflow (Fig. 3A) could be a major hazard in the valley if it were to become more active. Some mass-wasting, including slump earthflows and debris flows, may be related to earthquakes in the region (Zhang and Xu, 1993), an interpretation supported by increases in landslide frequency after both the 2008 Wenchuan and 2017 Jiuzhaigou earthquakes (Han et al., 2018; Xie et al., 2018). Despite the fault running through or near Heye Catchment and long-recognized debris-flow hazards, a GIS-based landslide susceptibility analysis of Jiuzhaigou completed after the 2017 earthquake found that Heye Catchment is at low risk for landslides due to relatively low slope steepness as calculated using remotely sensed digital topographic data (Yi et al., 2019, 2020).

Terraces formed by slumping in the Heye Catchment contain the only known archaeological sites in Jiuzhaigou and the oldest site in the region, Ashaonao (d'Alpoim Guedes et al., 2015). Archaeological evidence from Ashaonao indicates that people occupied the region as early as 3.4 ka (d'Alpoim Guedes et al., 2015). Artifacts are concentrated in the paleosol and slightly above the paleosol in gravelly loess but are not found in the loess underlying the paleosol (Henck et al., 2010; Urgenson et al., 2014; d'Alpoim Guedes et al., 2015; Figs. 3 and 4).

Previous studies leave open several questions about the loess. There is uncertainty about when the younger loess deposited, whether and how it may have been modified syn- or postdeposition, and what role landsliding and human occupation may have played in any modification. Prior work on the younger, gravelly loess used radiocarbon dates of bulk charcoal, grain-size analyses of the loess (i.e., excluding the coarse lithic component), and rare earth element analysis at the Ashaonao archaeological site to determine that the loess is likely derived from fine-grained glaciofluvial deposits in eastern Tibet during the Late Holocene and was deposited continuously over the last ~5000 years (Wen et al., 2014, 2017), but considers neither the older loess nor the source of gravel in the younger loess. Henck et al. (2010) interpret the older loess below the paleosol as primary loess deposition, which they date to the late Pleistocene/Early Holocene (11.1 ± 0.7 and 18 ± 1.4 ka), and younger gravelly loess above the paleosol as material remobilized by Late Holocene landslides, with the gravel as having been incorporated during landsliding. Thus, three questions remain about the Heye Catchment loess: (1) What is the source of gravel in the younger loess? (2) Is the younger loess remobilized or primary deposition? (3) When were the two loesses deposited, and what inferences about Holocene climate can they support? Answers would provide insight to Holocene climate in the Jiuzhaigou region; how human habitation may have influenced the character of loess deposits; and how the loess, and the possible role of landsliding in modifying the loess, may have influenced human inhabitance.

METHODS

We conducted fieldwork in the summers of 2007, 2008, 2010, 2011, and 2016. In summer 2008, an archaeological team

https://doi.org/10.1017/qua.2022.44 Published online by Cambridge University Press

Figure 4. Catalogue ID 07JZGASN_37d. Fragments of a single ceramic vessel from T5. One of these fragments (unknown) is one of the dated sherds.

excavated the Ashaonao archaeological site (Lu et al., 2010; Urgenson et al., 2014; Harrell et al., 2017). In summer 2016, stratigraphy and detailed sections were drawn for seven terrace faces. In summer 2011, we described stratigraphy of 50 terrace scarps and collected charcoal samples for radiocarbon dating and sediment samples for grain-size analysis, thin sections, and optically stimulated luminescence (OSL) dating from 19 of those scarps. Twelve sampled scarps had loess exposed under a paleosol or gravelly loess; eight of these have <1.5 m of exposed loess. The remaining four scarps have between 3.5 and 5 m of exposed loess below a paleosol. While we collected samples from the entire section of the younger loess, we confined our geochronology sampling to the upper 2.8 m of the older loess and grain-size sampling to the upper 3.5 m of the older loess, which is locally up to 5 m thick. The one OSL sample collected deeper than 2.8 m in the older loess was damaged during shipment from China.

We used petrographic analysis to characterize mineralogy of the older loess and the younger, gravelly loess. We embedded in epoxy the sediment from seven samples from terraces HY49 and HY50 collected in the field in 2011, made thin sections from the epoxy-embedded sediment, and analyzed the polished thin sections using a petrographic microscope. To determine percentages of quartz, calcite, and mica, we point counted at least 475 grains from each sample and identified the grains as quartz, calcite, mica, or other.

We used radiocarbon dating of organic material and luminescence dating of sherds and sediments to determine the timing of loess deposition. Charcoal, grain, wood, or bone samples for radiocarbon dating (n = 32) were taken in 2011 and 2016 from anthropogenic layers, paleosols, and the younger loess unit and were analyzed at the University of California Irvine Keck Carbon Cycle Accelerator Mass Spectrometry Laboratory (2011 samples) (Southon and Santos, 2004, 2007; Southon et al., 2004) and at the Oxford Radiocarbon Accelerator Unit (2016 samples) (Ramsey et al., 2004; Brock et al., 2010). After pretreatment with weak HCl, carbon dioxide was extracted and then graphitized on an iron catalyst. We used AMS to measure the graphitized carbon dioxide for $^{14}C/^{12}C$ ratios. In addition to new radiocarbon ages, we include analysis of 27 previously published radiocarbon ages (Henck et al., 2010; d'Alpoim Guedes et al., 2015; Wen et al., 2017). We calibrated new and previously published radiocarbon ages to calendar years with CALIB v. 8.2 using the IntCal20 data set (Reimer et al., 2020; Stuiver et al., 2022). To facilitate comparison with luminescence ages, we report the probability weighted mean age in thousands of years (ka) before 1950 rather than a calendar date; error bars for these dates span the range reported by OxCal.

Sherds were collected in 2007 and bagged in the field along with small samples of surrounding sediment for radiation measurements. Sediment was sampled in 2011 in metal pipes, the ends of which were then stuffed with paper and sealed with dark tape. We dated sherds using thermoluminescence, infrared stimulated luminescence, and OSL at the University of Washington Luminescence Lab (see Fig. 4 for a photo of a representative sherd sample). We dated sediments using OSL on 4 mm aliquots of 63–90 μm quartz at the Desert Research Institute Luminescence Lab in Nevada using a modified single-aliquot regenerative dose approach (Murray and Wintle, 2000; see text in Supplementary Material and Supplementary Tables S1–S8 for more details). We also include previously reported luminescence ages for sediments in the Heye Catchment (Henck et al., 2010; Feathers et al., 2012). The ages reported by Henck et al. (2010) were revised in Feathers et al. (2012). The latter paper used fine grains (1–8 μm) for measurement and tried to isolate the quartz signal both by chemical treatment and by application of pulsing methods. Both methods produced similar ages. For this paper,

https://doi.org/10.1017/qua.2022.44 Published online by Cambridge University Press

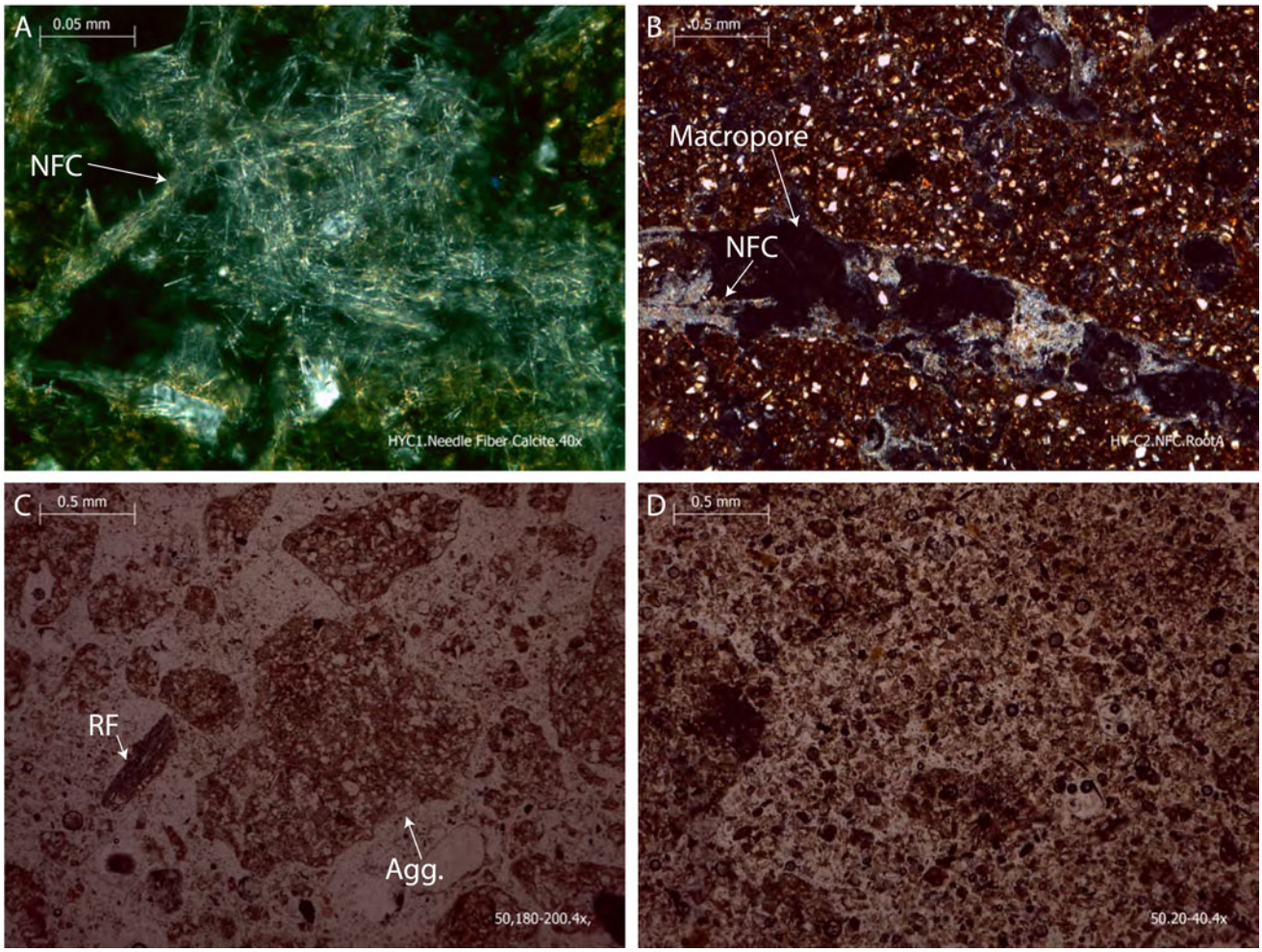

Figure 5. Transmitted-light thin-section micrographs of samples from Heye Catchment: (A and B) taken between crossed polarizers; (C and D) in plane-polarized light. (A) Intact section of the paleosol showing the needle-fiber calcite (labeled NFC). (B) Intact section of the paleosol showing needle fiber calcite (NFC) filling a macropore. (C) HY50 sample above the paleosol showing the lithics (RF) and aggregates (Agg.), which are coarser than quartz grains. (D) HY50 older loess sample below the paleosol.

we used the ages from the chemical treatment, because that is the same procedure used by the Desert Research Institute (except on larger grain sizes) for the new ages we report. However, it would not make a significant difference if we used the pulsed ages. The chemical treatment was not applied to three samples from Feathers et al. (2012), so we report the pulsed ages for these. To facilitate comparison with radiocarbon data, all OSL ages are reported in thousands of years (ka) before 1950.

To determine the grain-size distributions of the loess and gravelly loess in Heye Catchment, we collected 50 samples of sediment from 17 terraces, 35 samples of loess below the paleosol and 15 of gravelly loess above the paleosol. After pretreating sediment with hydrogen peroxide to remove organics, we used a Mastersizer laser diffractometer at Whitman College, Walla Walla, Washington, USA, to quantify the grain-size distribution of the <2 mm fraction of samples.

Because all samples had multiple distinct modes, we used QGrain (Liu et al., 2021)—software that implements the methods described in Sun et al. (2004)—to separate grain-size distributions of mixed samples into component parts. QGrain implements a single-specimen unmixing (SSU) model that reports the mean, standard deviation, and fraction of the sample for a defined number of unimodal parametrically distributed component sources. This allows us to determine similarities and differences among samples without having to propose and measure grain-size distributions of possible source regions (Sun et al., 2004). Thus, while we are unable to identify specific source locations using the SSU model, we are able to determine whether different samples are mixtures of material from the same or different sources. QGrain allows the user to choose between normal and Weibull curve fits and to determine the number of components in the mixture. Prior work on CLP loess grain sizes suggests that Weibull distributions may be more appropriate for loess areas, because modern wind speeds have a Weibull distribution (Sun et al., 2004). However, all samples had good, statistically significant fits with normal distributions, and thus we used normal distributions rather than Weibull, which requires more parameters to be fit and therefore has the potential to overfit the data.

RESULTS

Mineralogy and petrography

In thin section, loess samples from both the older and younger loess units are composed of individual grains that grade from

https://doi.org/10.1017/qua.2022.44 Published online by Cambridge University Press

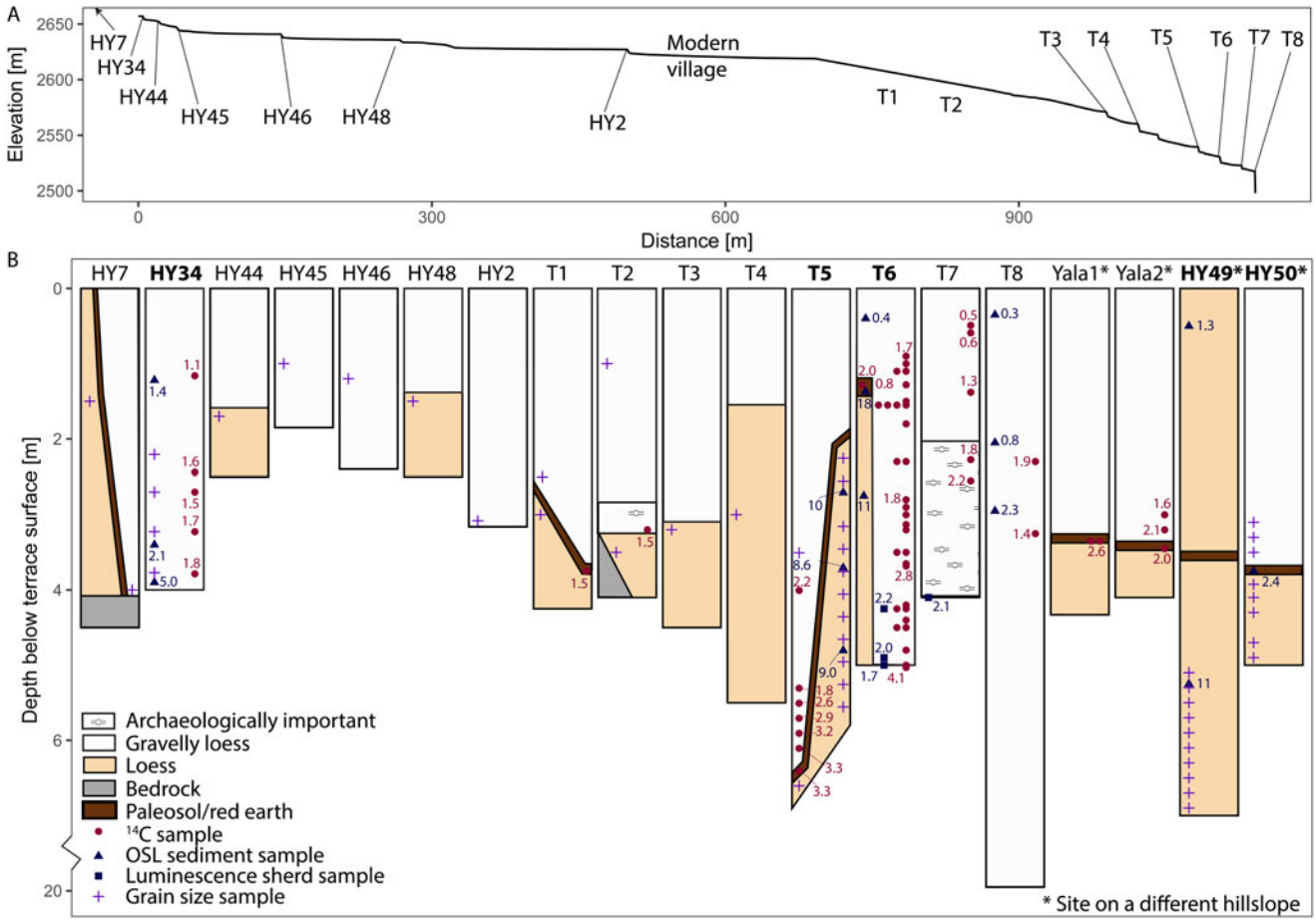

Figure 6. Overview of stratigraphy, sample locations, and geochronology. (A) Longitudinal profile across the main study area with terraces labeled. HY7 is uphill of HY34, but profile is not available. T1 and T2 are not captured in the longitudinal profile, but approximate location is noted. (B) Stratigraphy of terraces and locations of samples shown. Selected dates are provided (in ka). Details on all data included are in Supplementary Tables S9 and S10. The Ashaonao excavation was at T6. Location of terraces is in Fig. 1.

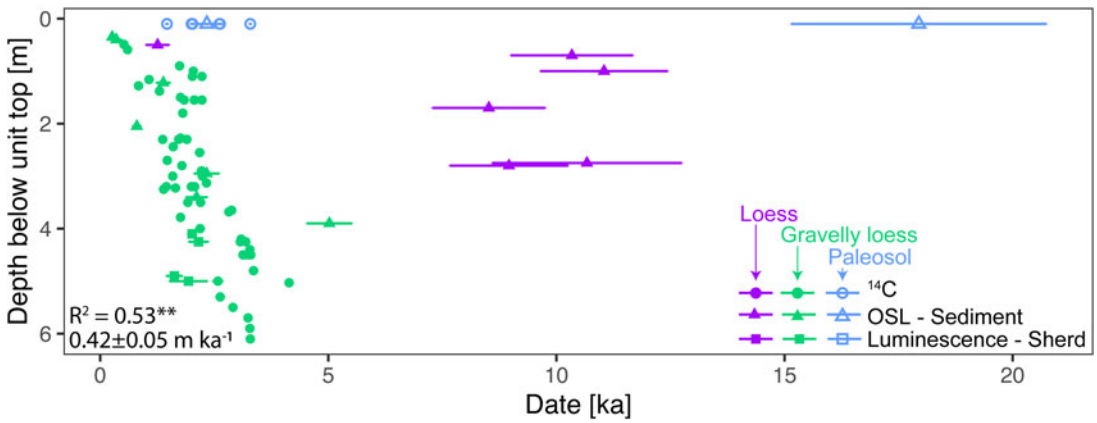

Figure 7. All ages as a function of depth below stratigraphic surface (i.e., terrace top for gravelly loess and either terrace top or paleosol for loess, depending on stratigraphy of the terrace). 2σ error bars are shown; some are smaller than the symbols used and not visible. Dates with ages >5.1 ka and samples taken from the paleosol were not used in the correlation analysis for date as a function of depth. Data shown includes previously published OSL and ^{14}C data for terraces in Heye Catchment (Henck et al., 2010; Feathers et al., 2012; Wen et al., 2014, 2017; d'Alpoim Guedes et al., 2015). Details of all ages shown are in Supplementary Tables S9–S12. $^{**}p < 0.01$.

rounded to subangular. The younger, gravelly loess also contains aggregates of loess particles, lithics, and needle-fiber calcite (Fig. 5C). The older loess samples only contain individual rounded particles and no soil aggregates (Fig. 5D). The composition of older loess is >60% quartz, 8–15% mica, 8–13% calcite, and up to 24% other minerals. The composition of younger gravelly loess is ~50% quartz, ~20% metamorphic lithics, 7–10% mica (muscovite and biotite), 5–13% calcite, and up to 18%

https://doi.org/10.1017/qua.2022.44 Published online by Cambridge University Press

other minerals. Pedogenic aggregates are common in the younger, gravelly loess samples taken from all depths of the terrace scarps. Both lithics and aggregates are coarser than grains of primary minerals. Lithics consist of angular fragments of metamorphic rock that have lithologies consistent with having been derived from the bedrock exposed in road cuts and landslide scarps in the Heye Catchment. Younger gravelly loess from samples taken in or slightly above the paleosols have fragments of needle-fiber calcite, a distinctive texture composed of porous masses of acicular calcite crystals in subparallel orientations. In thin sections made of a sample of the paleosol (HY-C), needle-fiber calcite is found in voids that appear to be macropores formed by roots (Fig. 5A and B).

Geochronology

Radiocarbon and luminescence ages of sediment and pottery sherds, including those from previous studies of Heye loess and terraces (Henck et al., 2010; Feathers et al., 2012; d'Alpoim Guedes et al., 2015; Wen et al., 2017), fall into two distinct age groups: those from the younger loess are younger than 5.1 ka, and those from the older loess are older than 8 ka (Figs. 6 and 7, Supplementary Fig. S11, Supplementary Tables S9–S12). The paleosol, stratigraphically located between the older and younger loess, yielded dates that fall within the age ranges of both the older and younger loess units, reflecting that the paleosols consist of older loess parent material and younger organics, sediments, and artifacts incorporated over the period of paleosol formation. Thus, we group ages from the paleosol separately from those from the two loess units. The single anomalously old age of paleosol material is likely the age of the older loess parent material, while the younger ages are likely the age of charcoal and sediments incorporated into the older loess during the hiatus in loess deposition.

Ages of material sampled from young loess linearly increase with depth below the current terrace surface (Fig. 7) and indicate a deposition rate of 0.39 ± 0.05 m/ka. Four sherd dates fall within this trend, implying that the sherds were buried relatively quickly after the pottery was fired. In contrast to the younger loess, the large uncertainties of OSL ages of the older loess preclude defining an age–depth relationship; five samples have statistically indistinguishable ages from 11.1 to 8.58 ka (Fig. 7); the error-weighted mean deposition age of the older loess (excluding the outlier paleosol sample) is 9.6 ± 1.6 ka. The 11–8.6 ka age range for a 2.8 m section of loess could suggest relatively rapid loess deposition, but we cannot determine this with the data available. Because our older loess ages extend to no more than 2.8 m below the surface on deposits up to 5 m thick, we may only have ages for the most recent ~50% of the period of loess deposition and cannot determine the date for onset of loess deposition.

Grain size

Analysis of grain-size data indicates there are multiple components of the Heye loess but that the number of components and relative dominance differs between the younger loess, the upper part of the older loess, and the lower part of the older loess (Figs. 8 and 9, Supplementary Fig. S12, Supplementary Tables S13–S15). The coarse (33–49 μm), medium (6.4–10.5 μm), and fine (0.58–0.71 μm) components are the first, second, and third most dominant components of the younger loess, upper part of the older loess, and lower part of the older loess. However, the lower older loess has more coarse material and less medium and fine material than the upper older loess and younger loess. The younger loess and the upper older loess additionally have a very coarse (316–405 μm) component, and the younger loess also has a very fine (0.038–0.042 μm) component. The mean grain size and fraction of the sample contained in each component are consistent with depth for each of the stratigraphic units (younger loess, upper older loess, and lower older loess). However, the grain size and fraction of sample for a given component differ in the lower older loess compared with the younger loess and upper older loess (Fig. 9).

DISCUSSION

We characterized the petrography and grain size for an older and a younger Holocene loess from Heye Catchment, Jiuzhaigou, and used radiocarbon to age charcoal and luminescence to age loess and sherds. In this section, we use the timing of deposition to make inferences about the regional Holocene climate, use grain-size data to infer paleowind conditions, and propose an explanation for the gravel component of the younger loess unit in Heye Catchment. Finally, we explore the environmental–social linkages suggested by the timing of loess deposition, landsliding, and human settlement in the Heye Catchment.

Timing of loess deposition and regional climate implications

Prior studies restricted their attention to the younger of the two loess units (Wen et al., 2014) or provided a provisional estimate for the depositional period for an older loess (Henck et al., 2010; Wen et al., 2017); dates in this study indicate that loess in Heye Catchment deposited in two distinct periods in the Holocene, >11–8.6 ka and 5.1–0.3 ka (Fig. 7), with a break in deposition and commensurate soil formation that corresponds to the MHCO. Because our samples of the older loess unit were restricted to the upper 2.8 m, we cannot define the onset of deposition. Prior studies also left unresolved whether, or how, the younger loess had been subject to syn- or postdepositional modification (Henck et al., 2010); the linear age–depth relationship derived from the younger loess across 11 terraces in the study area suggests the younger loess represents primary loess deposition that started ~5 ka. This conclusion is also supported by an exposure of young loess, above the paleosol, that does not contain gravel (HY49). Thin-section analysis of angular rock fragments contained within the loess show that these rocks have lithologies consistent with the local bedrock; later, we propose a mechanism by which these rock fragments could have been added to the depositing loess rather than being incorporated into remobilized loess.

The older loess (>11–8.6 ka) below the paleosol was deposited during a regional cool and dry period when loess was being deposited elsewhere in western China at least as early as 12 ka (Porter, 2001). Closer to Heye, pollen data from the Zoige area, 150 km northwest of Heye Catchment, indicate that the area alternated between woodland and grassland catchment between 10.3 and 7.3 ka (Zhao et al., 2011), suggesting intermittently colder conditions. In addition, several sites in the eastern TP record cool periods around 10 to 9.5 ka (Mischke and Zhang, 2010; Wang et al., 2010) and a temporal minimum in moisture on the TP around 9 ka (Ran and Feng, 2013) that corresponds to increased fire frequency (Sun et al., 2016; Zhao et al., 2017). Thus, loess in the Heye Catchment from >11–8.6 ka deposited

https://doi.org/10.1017/qua.2022.44 Published online by Cambridge University Press

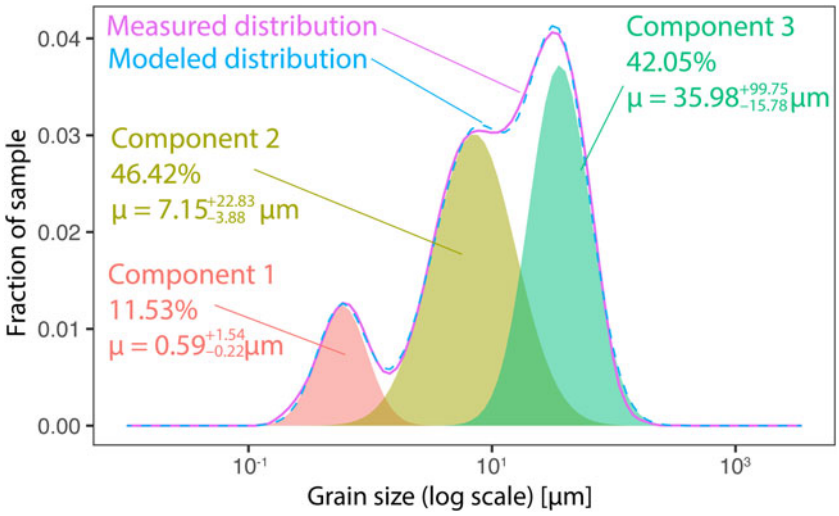

Figure 8. Example of a grain-size distribution for one sample, the three components, and the sum of the components as determined from QGrain. Each component is a lognormal distribution with the reported mean and standard deviation. Because the distributions are lognormal, the standard deviation is not symmetric in linear space. The mixture of the three lognormal distributions in the proportions noted on the figure sum to best approximate the measured distribution of this sample. Similar curves are available for all grain-size distributions analyzed in Supplementary Fig. S12.

during a regionally cool and dry period, as in the TP and the CLP. The timing of the cool and dry period on the CLP is no earlier than 12 ka, suggesting that we capture most of the period of Early Holocene deposition with the samples we measured.

There is a hiatus in the loess record in the Heye Catchment from 8.6–5.1 ka, more similar to the loess record in the TP, where loess deposition stops, than in the CLP, where loess deposition continues, albeit at a slower rate, through this period. The hiatus in loess deposition in the Heye Catchment corresponds to the MHCO, a warm period marked in western China by a slowing or hiatus in loess deposition; increased rates of soil formation, depending on the location (An et al., 1991; Porter, 2001); higher lake levels (Zhou et al., 1991); and reduced fire frequency (Sun et al., 1998; Huang et al., 2006). There is regional variability in MHCO timing, with the onset of the MHCO in western China and the TP occurring between 10 and 7.5 ka and the end occurring between 5 and 4 ka (An et al., 2000, 2006; Lehmkuhl et al., 2000; Feng et al., 2006; Wu et al., 2007; Zhu et al., 2009; Schütt et al., 2010; Bird et al., 2014). It is unclear whether the variability is systematic or due to different responses recorded in different climate proxies. Meta-analyses of regional data suggest that the MHCO is associated with an expansion of the Indian summer monsoon (An et al., 2006). The gradual expansion of the range of the Indian summer monsoon could well explain variations in timing of the MHCO around the region. Although the onset of the MHCO seems to vary somewhat, all of these core data suggest that the warm and wet period ended after 5 ka.

Closer to our study area, pollen and charcoal data from cores in two peat bogs 150 km northwest of Jiuzhaigou on the eastern edge of the TP indicate a warm and wet period from 10.8–5.7 ka (Hong et al., 2003; An et al., 2006; Zhao et al., 2011). These data suggest that the warm and wet period started as much as 2 ka earlier on the eastern TP than in Jiuzhaigou, but as with the regional data, it is possible that different climate proxies have different response times to the changing climate. Overall, the period of paleosol formation associated with a hiatus in loess deposition that we identify as dating from 8.6–5.1 ka suggest that climate conditions in the Heye Catchment may have been similar to those of the TP.

Resumption of loess deposition in the Heye Catchment corresponds to a post-MHCO cooling and drying regionally (An et al., 2000; Feng et al., 2006) and locally (Hong et al., 2003; An et al., 2006; Zhao et al., 2011; Wen et al., 2017); loess deposition in western China increased in 6–3 ka (Lehmkuhl et al., 2000, 2014; Porter, 2001; Huang et al., 2002; Maher et al., 2003; An et al., 2006; Stauch et al., 2012). On the eastern TP, multiproxy analyses of lake and peat cores corroborate cooling and drying after 6–3.7 ka (Zhang and Mischke, 2009; Zhao et al., 2011; Chen et al., 2014), with a slight warming after 3.7 ka (Zhang and Mischke, 2009), which we cannot evaluate in our data, because we have only two dates in younger loess that are older than 3.7 ka. Closer to Jiuzhaigou, cores of peat bogs to the west indicate a cool and dry climate after 5 ka (An et al., 2006). Overall, the climatic evidence in the region suggests that cool and dry conditions prevailed after 5 ka, when the younger Jiuzhaigou loess was deposited.

The deposition rate of the younger loess in Heye Catchment (0.39 ± 0.05 m/ka) may be inflated by human activity, a phenomenon documented elsewhere in China, because agriculture and land clearing increase erosion on uphill slopes and thus mobilize material deposited on loess deposits (Roberts et al., 2001). Because archaeological evidence suggests farmers arrived in Heye Catchment relatively soon after the younger loess started to accumulate (d'Alpoim Guedes et al., 2015), it is possible that farming accelerated loess deposition by redistributing material, including loess as well as locally derived sand and gravel, that sloughed from terrace scarps.

Paleowind conditions and loess sources

Although grain-size analyses identify three to five unique components of loess, we interpret three distinct sources and associated transport mechanisms for this material. The coarse fraction, which is present in all samples, has a mean grain size (44 ± 4 μm) that corresponds to grain sizes previously described as locally sourced material transported tens of kilometers (20–65 μm) during discontinuous events such as dust storms (Patterson and Gillette, 1977; Sun et al., 2004; Vandenberghe, 2013).The larger proportion of this sized material in lower older loess implies that surface winds were stronger during the Early Holocene when the lower older loess was deposited. The high westerly winds seem to have transported sediment through the entire period of loess deposition. High westerly winds likely transported the fine and medium (< ~10 μm) material, as has been

https://doi.org/10.1017/qua.2022.44 Published online by Cambridge University Press

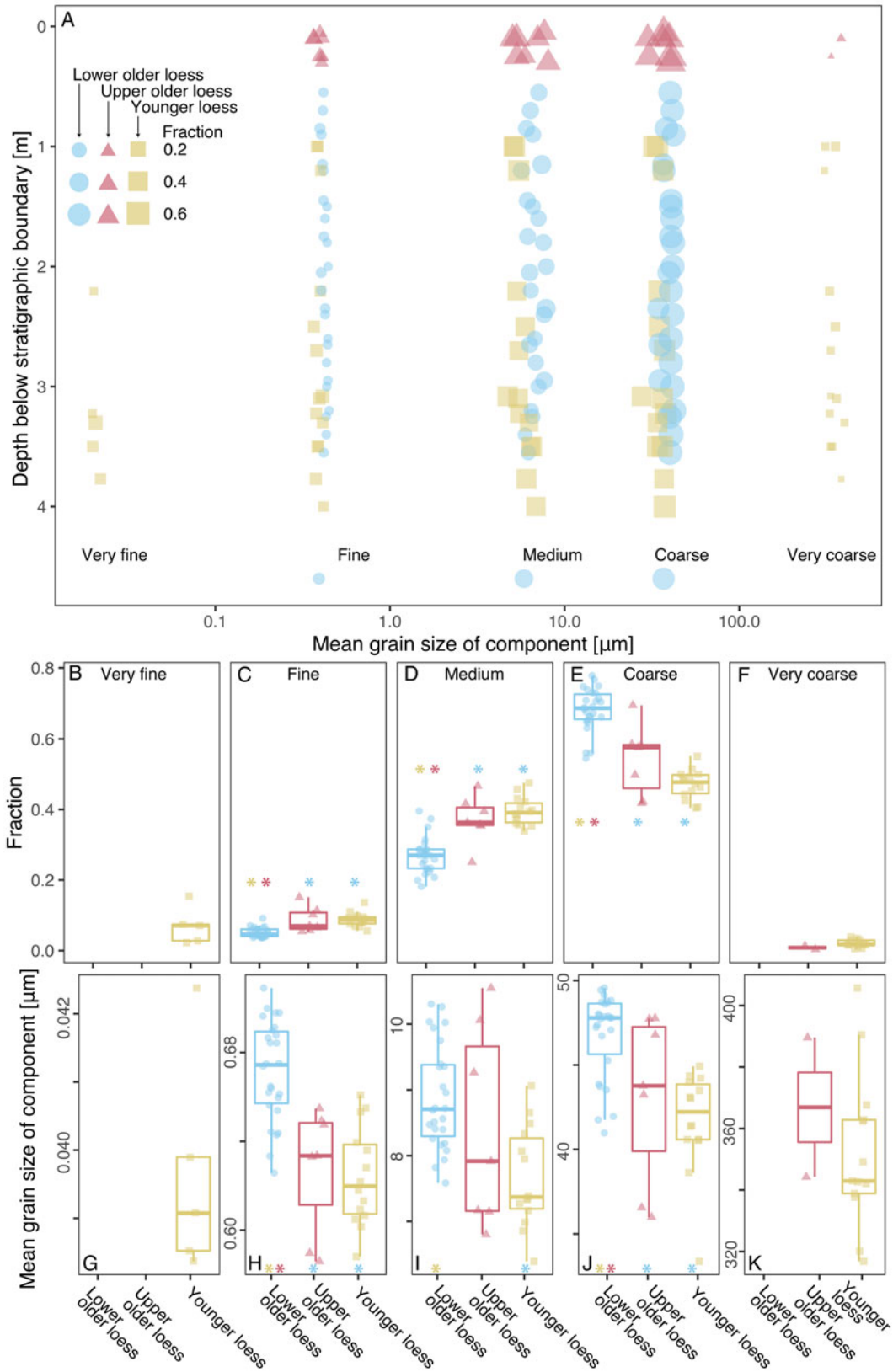

Figure 9. Variations in peak grain sizes and fractions of samples. (A) Mean peak size as a function of depth below the stratigraphic boundary for all samples. Shape size indicates fraction of the sample contained in each peak. (B–F) Box plots with overlying jitters showing variability in fraction of sample contained in each peak. Samples are grouped by stratigraphic unit (lower loess, upper loess in the top 30 cm, and gravelly loess). An asterisk (*) above a box plot indicates that distribution of fraction of sediment contained in the peak for the stratigraphic unit shown in the box plot is statistically significantly ($p < 0.05$) from the unit with the same color as the star for the peak shown. (G–K) mean grain size for each peak shown as a box plot with overlying jitters for each stratigraphic unit. An asterisk (*) at bottom as described for B–F. Center line is the median for box plots. Box boundaries extend to 25th and 75th percentiles. Whiskers are 1.5 times the interquartile range and outliers (not shown) are beyond that range.

https://doi.org/10.1017/qua.2022.44 Published online by Cambridge University Press

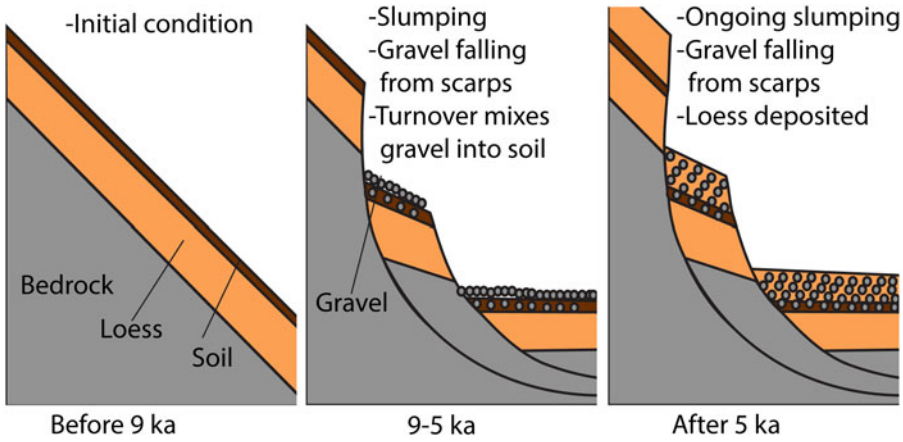

Figure 10. Conceptual model of how and when gravel became incorporated into loess in Heye Catchment.

inferred from similar data elsewhere in China (Sun et al., 2004). Finally, the very coarse fraction is too coarse to be transported by wind, even during discontinuous events (Patterson and Gillette, 1977; Sun et al., 2004; Vandenberghe, 2013). Thus, we conclude that this fraction is sourced from local bedrock during the same events that incorporated gravel into the younger loess.

Where did the gravel come from?

The existence of slump-block topography during deposition of the younger loess provides a mechanism for the incorporation into the younger loess of gravel and smaller lithics. Bedrock fragments mobilized by ravel and other modes of failure of the bedrock exposed at the base of some slump-block scarps would have fallen onto the relatively horizontal surfaces of slump blocks. As the loess accumulated, these locally derived lithics would then have been incorporated into the loess through bioturbation, pedogenesis, and farming (Fig. 10). As far as we know, a gravelly, lithic-rich loess such as this has not been documented elsewhere.

In Heye Catchment, deep-seated slumping produces failure planes through both loess and bedrock. This manner of slumping has apparently not been documented in other loess areas (see review by Li and Mo, 2019). Loess elsewhere in China experiences a range of landslide types that are attributed to both natural (Dijkstra et al., 1994; Wen et al., 2005; Zhang and Wang, 2007) and anthropogenic causes (Henck et al., 2010; Li and Mo, 2019). However, rotational slides previously documented in Chinese loess typically only involve the loess deposit itself, while documented landslides that also involve underlying bedrock are typically fast and have a long run-out (see review by Li and Mo, 2019).

That gravel is found incorporated into the paleosol at most exposures and paleosols formed during the period of nondeposition in Heye (8.6–5.1 ka) that corresponds with the MHCO indicates the slumping likely started during the MHCO. The MHCO's warmer and wetter climate (An et al., 2006) would have promoted slumping, including involvement of the weak bedrock underlying the Early Holocene loess. However, it is also possible that the development of slumping was driven by activity of local faults and by the weighting of the slope by the younger Holocene loess. Slumping that exposes bedrock is the only source of local gravel to incorporate into the loess, and thus the only explanation we have for gravel in the younger loess. Similarly, the absence of gravel in the older loess provides a limiting date of approximately 9 ka for the onset of slumping. Field evidence of active ground deformation indicates the slump feature is active; whether its activity has been continuous or episodic is unknown, but persistent activity over long time periods is characteristic of slump earthflow around the world (Bovis and Jones, 1992; Mackey et al., 2009; Rutter and Green, 2011; Coe, 2012; Handwerger et al., 2013).

Implications for the history of human inhabitance

The earliest evidence for occupation of the Ashaonao site dates to 3.4 ka (d'Alpoim Guedes et al., 2015), while slumping likely started earlier than 4.1 ka based on the presence of gravel in loess of that age. The occupants of the Ashaonao site arrived after the slump terraces formed and during the subsequent deposition of the younger loess; the oldest date of occupation postdates the oldest dates of gravelly loess. This raises the possibility that the occupants of the Ashaonao site settled there because of the topography created by the slumping as well as the preference for farming on loess soils (Henck et al., 2010; Schmidt et al., 2017). The documented use of wheat and barley at the Ashaonao site (d'Alpoim Guedes et al., 2015) provides further evidence of the site having been viewed as a favorable location for agriculture. The upper older loess is closer in grain-size distribution to the younger loess than the lower older loess. However, both the large gap of time between the older and younger loess deposits and the statistically identical ages of the older loess make it unlikely that there was a smooth transition in climate from the time of the lower and upper older loess. Thus, it seems unlikely that the upper older loess was deposited under different environmental conditions than the lower older loess. However, agricultural activity mixes soils, and thus it is possible that tilling for agriculture mixed younger loess into the upper 30 cm of the upper older loess. Abandonment of the site by ~2 ka (d'Alpoim Guedes et al., 2015) has not been explained; however, a reactivation of slump failure planes provides a possible explanation.

CONCLUSIONS

Loess in Heye Catchment deposited during cool and dry climate from >11 to 8.6 ka, was interrupted during the warmer and wetter MHCO (~8.6–4.1 ka), and resumed in the cooler and drier Late Holocene (<4.1 ka). The loess is a mixture of material of three

https://doi.org/10.1017/qua.2022.44 Published online by Cambridge University Press

to five grain-size distributions. The fine and medium distributions (<~10 μm) likely derive from transport by high westerly winds, the coarse distribution (~45 μm) may be windblown material sourced from the eastern TP, and the very coarse fraction is probably fragments of the local bedrock sourced from slump blocks and incorporated into the upper older loess and younger loess by gravity and farming. The relatively large fraction of the coarse grain-size fraction present in the older loess, exclusive of the upper 30 cm of that unit, suggests that the regional winds transporting material from the eastern TP were stronger during the Early Holocene loess deposition (>11–8.6 ka) than during the later Holocene deposition (<5.1 ka). The Late Holocene (<5.1 ka) loess was mixed with gravel sourced from local bedrock exposed in slump scarps; wetter conditions during the MHCO may have contributed to the slumping that formed the slump-block risers that are the presumed source for gravel in the younger loess. Archaeologically important stratigraphic layers in the gravelly loess suggest that human occupation of the site started soon after the Late Holocene loess deposition began, possibly due to the attractive combination of low angle surfaces created by the slump terraces and the loess soils.

Acknowledgments. The authors thank C. Suhr, P. Manley, and C. Dunn for running some of the grain-size analyses; S. Lugli for providing thin sections of the paleosol; N. McMillion for making the loess and gravelly loess thin sections; and Y. M. Liu for assistance with QGrain. We thank A. Corbett, A. Lubeck, J. Southon, C. Bertrand, H. Martinez, and other staff from the UC Irvine Keck Radiocarbon Lab for assistance in preparing and analyzing radiocarbon samples. We thank K. X. Goh, J. Schmidt, and the staff of the Jiuzhaigou National Nature Reserve Science Office for field assistance. The article benefited from conversations with R. Sletten, C. Schreiber, and S. Lugli.

Funding. The authors acknowledge funding from the Mellon Mayes Undergraduate Fellowship Program to DF, National Science Foundation BCS-1632207 to JdG and AH, National Geographic and Chiang Jing Kuo Foundation funding to JdG, a Natural Science Foundation of China postdoctoral fellowship and a Fulbright Student Fellowship to AHS, and a Program of Introducing Talents of Discipline to Universities (B08037) grant to YT.

Supplementary Material. The supplementary material for this article can be found at https://doi.org/10.1017/qua.2022.44

REFERENCES

An, C.-B., Feng, Z.-D., Barton, L., 2006. Dry or humid? Mid-Holocene humidity changes in arid and semi-arid China. *Quaternary Science Reviews* **25**, 351–361.

An, C.-B., Tang, L., Barton, L., Chen, F.-H., 2005. Climate change and cultural response around 4000 cal yr BP in the western part of Chinese Loess Plateau. *Quaternary Research* **63**, 347–352.

An, Z., Porter, S.C., Kutzbach, J.E., Wu, X., Wang, S., Liu, X., Li, X., Zhou, W., 2000. Asynchronous Holocene optimum of the East Asian monsoon. *Quaternary Science Reviews* **19**, 743–762.

An, Z.S., Kukla, G., Porter, S.C., Xiao, J.L., 1991. Late Quaternary dust flow on the Chinese Loess Plateau. *Catena* **18**, 125–132.

Bird, B.W., Polisar, P.J., Lei, Y., Thompson, L.G., Yao, T., Finney, B.P., Bain, D.J., Pompeani, D.P., Steinman, B.A., 2014. A Tibetan lake sediment record of Holocene Indian summer monsoon variability. *Earth and Planetary Science Letters* **399**, 92–102.

Bovis, M.J., Jones, P., 1992. Holocene history of earthflow mass movements in south-central British Columbia: the influence of hydroclimatic changes. *Canadian Journal of Earth Sciences* **29**, 1746–1755.

Brock, F., Higham, T., Ditchfield, P., Ramsey, C.B., 2010. Current pretreatment methods for AMS radiocarbon dating at the Oxford Radiocarbon Accelerator Unit (ORAU). *Radiocarbon* **52**, 103–112.

Burchfiel, B.C., Chen, Z., 2012. *Tectonics of the Southeastern Tibetan Plateau and Its Adjacent Foreland*. Geological Society of America Memoir 210.

Chen, B., Zheng, Z., Huang, K., Zheng, Y., Zhang, G., Zhang, Q., Huang, X., 2014. Radionuclide dating of recent sediment and the validation of pollen-environment reconstruction in a small watershed reservoir in southeastern China. *Catena* **115**, 29–38.

Coe, J.A., 2012. Regional moisture balance control of landslide motion: Implications for landslide forecasting in a changing climate. *Geology* **40**, 323–326.

Cui, P., Chen, X.Q., Liu, S.Q., Tang, B.X., 2007. Techniques of debris flow prevention in national parks. *Earth Science Frontiers* [online English edition] **14**, 172–177.

Cui, P., Liu, S., Tang, B., Chen, X., 2003. Debris flow prevention pattern in national parks—taking the world natural heritage Jiuzhaigou as an example. *Science in China, series E* **46**, 1–11.

d'Alpoim Guedes, J.A., Lu, H.L., Hein, A.M., Schmidt, A.H., 2015. Early evidence for the use of wheat and barley as staple crops on the margins of the Tibetan Plateau. *Proceedings of the National Academy of Sciences USA* **112**, 5625–5630.

Derbyshire, E., 1982. On the morphology, sediments and origins of the Loess Plateau of Central China. *Journal of the Geological Society of London* **139**, 172–194.

Derbyshire, E., 2001. Geological hazards in loess terrain, with particular reference to the loess regions of China. *Earth-Science Reviews* **54**, 231–260.

Derbyshire, E., Meng, X.M., Kemp, R.A., 1998. Provenance, transport and characteristics of modern aeolian dust in western Gansu Province, China, and interpretation of the Quaternary loess record. *Journal of Arid Environments* **39**, 497–516.

Dietze, E., Hartmann, K., Diekmann, B., Ijmker, J., Lehmkuhl, F., Opitz, S., Stauch, G., Wünnemann, B., Borchers, A., 2012. An end-member algorithm for deciphering modern detrital processes from lake sediments of Lake Donggi Cona, NE Tibetan Plateau, China. *Sedimentary Geology* 243–244, 169–180.

Dijkstra, T., Rogers, C., Smalley, I., Derbyshire, E., Li, Y.J., Meng, X.M., 1994. The loess of north-central China: geotechnical properties and their relation to slope stability. *Engineering Geology* **36**, 153–171.

Feathers, J.K., Casson, M.A., Henck, A., Chithambo, M.L., 2012. Application of pulsed OSL to polymineral fine-grained samples. *Radiation Measurements* **47**, 201–209.

Feng, Z.-D., An, C., Wang, H., 2006. Holocene climatic and environmental changes in the arid and semi-arid areas of China: a review. *The Holocene* **16**, 119–130.

Folk, R.L., 1980. *Petrology of Sedimentary Rocks*. Hemphill Publishing, Austin, TX.

Guo, J.J., Yang, G., Cao, J., Chen, B., Song, Y., Zhang, H.L., Lu, Z.M., Cai, Y.S., An, D.J., 2006. Jiuzhai—Huanglong Core Protected Area geology environmental investigations report. [In Chinese]. In: Jiang, Y.S. (Ed.). *Sichuan Provincial Geologic Investigation Team Report*. Sichuan Provincial Geologic Investigation Team, [Chengdu, Sichuan, China], p. 202.

Handwerger, A.L., Roering, J.J., Schmidt, D.A., 2013. Controls on the seasonal deformation of slow-moving landslides. *Earth and Planetary Science Letters* **377**, 239–247.

Han, L., Cheng, J., An, Y., Fang, L., Jiang, C., Chen, B., Wu, Z., Liu, J., Xu, X., Liu, R., 2018. Preliminary report on the 8 August 2017 M s 7.0 Jiuzhaigou, Sichuan, China, earthquake. *Seismological Research Letters* **89** (2A), 557–569.

Harrell, S., Yang, Q.X., Viraldo, S.J., Hagmann, R.K., Hinckley, T., Schmidt, A.H., 2017. Forest is forest and meadows are meadows: cultural landscapes and bureaucratic landscapes in Jiuzhaigou County, Sichuan. *Archiv Orientální* **84**, 595–623.

Henck, A., Taylor, J., Lu, H., Li, Y., Yang, Q., Grub, B., Breslow, S.J., *et al.*, 2010. Anthropogenic hillslope terraces and swidden agriculture in Jiuzhaigou National Park, northern Sichuan, China. *Quaternary Research* **73**, 201–207.

Hong, Y., Hong, B., Lin, Q., Zhu, Y., Shibata, Y., Hirota, M., Uchida, M., Leng, X., Jiang, H., Xu, H., 2003. Correlation between Indian Ocean summer monsoon and North Atlantic climate during the Holocene. *Earth and Planetary Science Letters* **211**, 371–380.

Huang, C.C., Pang, J.L., Chen, S.E., Su, H.X., Han, J., Cao, Y.F., Zhao, W.Y., Tan, Z.H., 2006. Charcoal records of fire history in the Holocene loess-soil sequences over the southern Loess Plateau of China. *Palaeogeography, Palaeoclimatology, Palaeoecology* **239**, 28–44.

Huang, C.C., Pang, J.L., Chen, S.E., Zhang, Z.P., 2003. Holocene dust accumulation and the formation of polycyclic cinnamon soils (luvisols) in the Chinese Loess Plateau. *Earth Surface Processes and Landforms* **28**, 1259–1270.

Huang, C.C., Pang, J.L., Huang, P., 2002. An early Holocene erosion phase on the loess tablelands in the southern Loess Plateau of China. *Geomorphology* **43**, 209–218.

Jiang, H.C., Ding, Z.L., 2010. Eolian grain-size signature of the Sikouzi lacustrine sediments (Chinese Loess Plateau): implications for Neogene evolution of the East Asian winter monsoon. *Geological Society of America Bulletin* **122**, 843–854.

Kuster, Y., Hetzel, R., Krbetschek, M., Tao, M.X., 2006. Holocene loess sedimentation along the Qilian Shan (China): significance for understanding the processes and timing of loess deposition. *Quaternary Science Reviews* **25**, 114–125.

Lacroix, P., Dehecq, A., Taipe, E., 2020. Irrigation-triggered landslides in a Peruvian desert caused by modern intensive farming. *Nature Geoscience* **13**, 56–60.

Lehmkuhl, F., Klinge, M., Rees-Jones, J., Rhodes, E.J., 2000. Late Quaternary aeolian sedimentation in central and south-eastern Tibet. *Quaternary International* **68**, 117–132.

Lehmkuhl, F., Owen, L.A., 2005. Late Quaternary glaciation of Tibet and the bordering mountains: a review. *Boreas* **34**, 87–100.

Lehmkuhl, F., Schulte, P., Zhao, H., Hulle, D., Protze, J., Stauch, G., 2014. Timing and spatial distribution of loess and loess-like sediments in the mountain areas of the northeastern Tibetan Plateau. *Catena* **117**, 23–33.

Lei, X., 1998. *Grain-size analysis and genesis of loess in the Qinling Mountains. Acta Geologica Sinica* 2, 9.

Liu, T.S., Ding, Z.L., 1998. Chinese loess and the paleomonsoon. *Annual Review of Earth and Planetary Sciences* **26**, 111–145.

Liu, Y., Liu, X., Sun, Y., 2021. QGrain: An open-source and easy-to-use software for the comprehensive analysis of grain size distributions. *Sedimentary Geology* **423**, 105980.

Li, Y., Mo, P., 2019. A unified landslide classification system for loess slopes: a critical review. *Geomorphology* **340**, 67–83.

Lowdermilk, W.C., 1924. Erosion and floods in the Yellow River watershed. *Journal of Forestry* **22**, 11–18.

LP DAAC, 2001. ASTER GDEM. In: NASA Land Processes Distributed Active Archive Center (Ed.), USGS/Earth Resources Observation and Science (EROS) Center, Sioux Falls, SD.

Lu, H., Henck, A., Taylor, J., Li, Y., 2010. *Archaeological Research at a Han Dynasty Settlement in Jiuzhaigou National Park, Sichuan*. Society for American Archaeology, St. Louis, MO.

Mackey, B.H., Roering, J.J., McKean, J.A., 2009. *Long-term kinematics and sediment flux of an active earthflow*, Eel River, California. Geology **37**, 803–806.

Maher, B.A., Hu, M., Roberts, H.M., Wintle, A.G., 2003. Holocene loess accumulation and soil development at the western edge of the Chinese Loess Plateau: implications for magnetic proxies of palaeorainfall. *Quaternary Science Reviews* **22**, 445–451.

Maher, B.A., Mutch, T.J., Cunningham, D., 2009. Magnetic and geochemical characteristics of Gobi Desert surface sediments: implications for provenance of the Chinese Loess Plateau. *Geology* **37**, 279–282.

Mischke, S., Zhang, C., 2010. Holocene cold events on the Tibetan Plateau. *Global and Planetary Change* **72**, 155–163.

Murray, A.S., Wintle, A.G., 2000. Luminescence dating of quartz using an improved single-aliquot regenerative-dose protocol. *Radiation Measurements* **32**, 57–73.

Nottebaum, V., Lehmkuhl, F., Stauch, G., Hartmann, K., Wünnemann, B., Schimpf, S., Lu, H., 2014. Regional grain size variations in aeolian sediments along the transition between Tibetan highlands and north-western Chinese deserts—the influence of geomorphological settings on aeolian transport pathways. *Earth Surface Processes and Landforms* **39**, 1960–1978.

Nottebaum, V., Stauch, G., Hartmann, K., Zhang, J., Lehmkuhl, F., 2015. Unmixed loess grain size populations along the northern Qilian Shan (China): relationships between geomorphologic, sedimentologic and climatic controls. *Quaternary International* **372**, 151–166.

Nugteren, G., Vandenberghe, J., 2004. Spatial climatic variability on the Central Loess Plateau (China) as recorded by grain size for the last 250 kyr. *Global and Planetary Change* **41**, 185–206.

Patterson, E.M., Gillette, D., 1977. Commonalities in measured size distributions for aerosols having a soil-derived component. *Journal of Geophysical Research* **82**, 2074–2082.

Porter, S.C., 2001. Chinese loess record of monsoon climate during the last glacial-interglacial cycle. *Earth-Science Reviews* **54**, 115–128.

Prins, M.A., Zheng, H., Beets, K., Troelstra, S., Bacon, P., Kamerling, I., Wester, W., Konert, M., Huang, X., Ke, W., 2009. Dust supply from river floodplains: the case of the lower Huang He (Yellow River) recorded in a loess–palaeosol sequence from the Mangshan Plateau. *Journal of Quaternary Science* **24**, 75–84.

Pullen, A., Kapp, P., McCallister, A.T., Chang, H., Gehrels, G.E., Garzione, C.N., Heermance, R.V., Ding, L., 2011. Qaidam basin and northern Tibetan Plateau as dust sources for the Chinese Loess Plateau and paleoclimatic implications. *Geology* **39**, 1031–1034.

Pye, K., 2015. *Aeolian Dust and Dust Deposits*. Academic Press, Orlando, FL.

Qiao, X., Du, J., Lugli, S., Ren, J., Xiao, W., Chen, P., Tang, Y., 2016. Are climate warming and enhanced atmospheric deposition of sulfur and nitrogen threatening tufa landscapes in Jiuzhaigou National Nature Reserve, Sichuan, China? *Science of the Total Environment* **562**, 724–731.

Qin, X., Cai, B., Liu, T., 2005. Loess record of the aerodynamic environment in the east Asia monsoon area since 60,000 years before present. *Journal of Geophysical Research: Solid Earth* **110**(B1). https://doi.org/10.1029/2004JB003131.

Ramsey, C.B., Higham, T., Leach, P., 2004. Towards high-precision AMS: progress and limitations. *Radiocarbon* **46**, 17–24.

Ran, M., Feng, Z., 2013. Holocene moisture variations across China and driving mechanisms: A synthesis of climatic records. *Quaternary International* **313**, 179–193.

Reimer, P.J., Austin, W.E.N., Bard, E., Bayliss, A., Blackwell, P.G., Bronk Ramsey, C., Butzin, M., *et al.*, 2020. The IntCal20 Northern Hemisphere Radiocarbon Age Calibration Curve (0–55 cal kBP). *Radiocarbon* **62**, 725–757.

Roberts, H.M., Wintle, A.G., Maher, B.A., Hu, M.Y., 2001. Holocene sediment-accumulation rates in the western Loess Plateau, China, and a 2500-year record of agricultural activity, revealed by OSL dating. *The Holocene* **11**, 477–483.

Rutter, E., Green, S., 2011. Quantifying creep behaviour of clay-bearing rocks below the critical stress state for rapid failure: Mam Tor landslide, Derbyshire, England. *Journal of the Geological Society of London* **168**, 359–372.

Schmidt, A.H., Li, Y.X., Tang, Y., 2017. Uninteded side effects of conservation: a case study of changing land use in Jiuzhaigou, Sichuan, China. *Mountain Research and Development* **37**, 56–65.

Schütt, B., Berking, J., Frechen, M., Frenzel, P., Schwalb, A., Wrozyna, C., 2010. Late Quaternary transition from lacustrine to a fluvio-lacustrine environment in the north-western Nam Co, Tibetan Plateau, China. *Quaternary International* **218**, 104–117.

Sheng, H., 2010. Zoige basin loess origin in the northern Tibetan Plateau. *Earth Science-Journal of China University of Geosciences* **35**, 62–74.

Southon, J., Santos, G., 2004. Ion source development at KCCAMS, University of California, Irvine. *Radiocarbon* **46**, 33–39.

Southon, J., Santos, G., Druffel-Rodriguez, K., Druffel, E., Trumbore, S., Xu, X., Griffin, S., Ali, S., Mazon, M., 2004. The Keck Carbon Cycle AMS laboratory, University of California, Irvine: initial operation and a background surprise. *Radiocarbon* **46**, 41–49.

Southon, J., Santos, G.M., 2007. Life with MC-SNICS. Part II: Further ion source development at the Keck carbon cycle AMS facility. *Nuclear Instruments and Methods in Physics Research, section B* **259**, 88–93.

Stauch, G., IJmker, J., Pötsch, S., Zhao, H., Hilgers, A., Diekmann, B., Dietze, E., Hartmann, K., Opitz, S., Wünnemann, B., 2012. Aeolian sediments on the north-eastern Tibetan Plateau. *Quaternary Science Reviews* **57**, 71–84.

Stevens, T., Palk, C., Carter, A., Lu, H., Clift, P.D., 2010. Assessing the provenance of loess and desert sediments in northern China using U-Pb dating and morphology of detrital zircons. *GSA Bulletin* **122**, 1331–1344.

Stuiver, M., Reimer, P.J., Reimer, R.W., 2022. CALIB 8.2 (accessed April 15, 2022). http://calib.org.

https://doi.org/10.1017/qua.2022.44 Published online by Cambridge University Press

Sun, D., Bloemendal, J., Rea, D.K., An, Z., Vandenberghe, J., Lu, H., Su, R., Liu, T., 2004. Bimodal grain-size distribution of Chinese loess, and its palaeoclimatic implications. *Catena* **55**, 325–340.

Sun, D., Shaw, J., An, Z., Cheng, M., Yue, L., 1998. Magnetostratigraphy and paleoclimatic interpretation of a continuous 7.2 Ma Late Cenozoic eolian sediments from the Chinese Loess Plateau. *Geophysical Research Letters* **25**, 85–88.

Sun, J., Li, S.-H., Muhs, D.R., Li, B., 2007. Loess sedimentation in Tibet: provenance, processes, and link with Quaternary glaciations. *Quaternary Science Reviews* **26**, 2265–2280.

Sun, J., Yue, H., Shen, Z., Fang, L., Zhan, Y., Sun, X., 2018. The 2017 Jiuzhaigou earthquake: a complicated event occurred in a young fault system. *Geophysical Research Letters* **45**, 2230–2240.

Sun, W., Zhang, E., Shen, J., Chen, R., Liu, E., 2016. Black carbon record of the wildfire history of western Sichuan Province in China over the last 12.8 ka. *Frontiers of Earth Science* **10**, 634–643.

Sun, Y., Lu, H., An, Z., 2000. Grain size distribution of quartz isolated from Chinese loess paleosol. *Chinese Science Bulletin* **45**, 2296.

Urgenson, L.S., Schmidt, A.H., Combs, J.K., Harrell, S., Hinckley, T.M., Yang, Q.X., Ma, Z.Y., Li, Y.X., Lu, H.L., MacIver, A., 2014. Traditional livelihoods, conservation and meadow ecology in Jiuzhaigou National Park, Sichuan, China. *Human Ecology* **42**, 481–491. 10.1007/s10745-014–9650-z.

Vandenberghe, J., 2013. Grain size of fine-grained windblown sediment: a powerful proxy for process identification. *Earth-Science Reviews* **121**, 18–30.

Vriend, M., Prins, M.A., 2005. Calibration of modelled mixing patterns in loess grain-size distributions: an example from the north-eastern margin of the Tibetan Plateau, China. *Sedimentology* **52**, 1361–1374.

Wang, H., Hong, Y., Lin, Q., Hong, B., Zhu, Y., Wang, Y., Xu, H., 2010. Response of humification degree to monsoon climate during the Holocene from the Hongyuan peat bog, eastern Tibetan Plateau. *Palaeogeography, Palaeoclimatology, Palaeoecology* **286**, 171–177.

Wang, Y.-s., Li, Y.-z., Xiang, F., 2003. The Ganzi loess origin in the west Sichuan Plateau. *Journal of Geomechanics* **9**, 96–96.

Wen, B.P., Wang, S., Wang, E., Zhang, J.M., Wu, Y.G., Wang, X., 2005. Deformation characteristics of loess landslide along the contact between loess and Neocene red mudstone. *Acta Geologica Sinica* [English edition] **79**, 139–151.

Wen, X., Chen, M., Feng, W., Huang, C., 2017. Mid-Late Holocene climatic changes recorded by loess deposits in the eastern margin of the Tibetan Plateau: implication for human migrations. *Quaternary International* **441**, 77–88.

Wen, X., Tang, Y., Huang, C.M., Gongbo, S.L., 2014. Multi-material source of loess deposits from the Jiuzhaigou National Nature Reserve on the eastern margin of the Tibetan Plateau. *Mountain Research* **32**, 603–614.

World Wildlife Fund, 2008. HydroSHEDS (accessed January 22, 2009). https://www.hydrosheds.org.

Wu, G., Zhang, C., Zhang, X., Tian, L., Yao, T., 2010. Sr and Nd isotopic composition of dust in Dunde ice core, northern China: implications for source tracing and use as an analogue of long-range transported Asian dust. *Earth and Planetary Science Letters* **299**, 409–416.

Wu, Y., Andreas, L., Bernd, W., Li, S., Wang, S., 2007. Holocene climate change in the Central Tibetan Plateau inferred by lacustrine sediment geochemical records. *Science in China, series D* **50**, 1548–1555.

Xiao, J., Chang, Z., Si, B., Qin, X., Itoh, S., Lomtatidze, Z., 2009. Partitioning of the grain-size components of Dali Lake core sediments: evidence for lake-level changes during the Holocene. *Journal of Paleolimnology* **42**, 249–260.

Xiao, J., Fan, J., Zhou, L., Zhai, D., Wen, R., Qin, X., 2013. A model for linking grain-size component to lake level status of a modern clastic lake. *Journal of Asian Earth Sciences* **69**, 149–158.

Xiao, J., Porter, S.C., An, Z.S., Kumai, H., Yoshikawa, S., 1995. Grain-size of quartz as an indicator of winter monsoon strength on the Loess Plateau of central China during the last 130,000-Yr. *Quaternary Research* **43**, 22–29.

Xie, Z., Zheng, Y., Yao, H., Fang, L., Zhang, Y., Liu, C., Wang, M., Shan, B., Zhang, H., Ren, J., 2018. Preliminary analysis on the source properties and seismogenic structure of the 2017 M s 7.0 Jiuzhaigou earthquake. *Science China Earth Sciences* **61**, 339–352.

Yang, S.L., Fang, X.M., Shi, Z.T., Lehmkuhl, F., Song, C.H., Han, Y.X., Han, W.X., 2010a. Timing and provenance of loess in the Sichuan basin, southwestern China. *Palaeogeography, Palaeoclimatology, Palaeoecology* **292**, 144–154.

Yang, S.L., Fang, X.M., Yan, M.D., Shi, Z.T., Song, C.H., Han, Y.X., 2010b. Grain size profiles in the Chengdu Clay, eastern margin of the Tibetan Plateau: implications for significant drying of Asia since similar to 500 ka BP. *Journal of Asian Earth Sciences* **38**, 57–64.

Yi, Y., Zhang, Z., Zhang, W., Jia, H., Zhang, J., 2020. Landslide susceptibility mapping using multiscale sampling strategy and convolutional neural network: a case study in Jiuzhaigou region. *Catena* **195**, 104851.

Yi, Y., Zhang, Z., Zhang, W., Xu, Q., Deng, C., Li, Q., 2019. GIS-based earthquake-triggered-landslide susceptibility mapping with an integrated weighted index model in Jiuzhaigou region of Sichuan Province, China. *Natural Hazards and Earth System Sciences* **19**, 1973–1988.

Zhang, C.J., Mischke, S., 2009. A Lateglacial and Holocene lake record from the Nianbaoyeze Mountains and inferences of lake, glacier and climate evolution on the eastern Tibetan Plateau. *Quaternary Science Reviews* **28**, 1970–1983.

Zhang, D., Xu, M., 1993. An approach to mass movements in the Jiuzhaigou catchment. *Natural Hazards* **8**, 141–151.

Zhang, D.X., Wang, G.H., 2007. Study of the 1920 Haiyuan earthquake-induced landslides in loess (China). *Engineering Geology* **94**, 76–88.

Zhang, M., 2019. *Impacts of Mountain Hazards on Sustainable Tourism Development in Sichuan, China*. PhD thesis, Environmental Science and Engineering Department, Sichuan University, Chengdu.

Zhang, X., An, Z., Chen, T., Zhang, G., Arimoto, R., Ray, B.J., 1994. Late Quaternary records of the atmospheric input of eolian dust to the center of the Chinese Loess Plateau. *Quaternary Research* **41**, 35–43.

Zhao, W., Zhao, Y., Qin, F., 2017. Holocene fire, vegetation, and climate dynamics inferred from charcoal and pollen record in the eastern Tibetan Plateau. *Journal of Asian Earth Sciences* **147**, 9–16.

Zhao, Y., Yu, Z.C., Zhao, W.W., 2011. Holocene vegetation and climate histories in the eastern Tibetan Plateau: controls by insolation-driven temperature or monsoon-derived precipitation changes? *Quaternary Science Reviews* **30**, 1173–1184.

Zhou, S.Z., Chen, F.H., Pan, B.T., Cao, J.X., Li, J.J., Derbyshire, E., 1991. Environmental change during the Holocene in western China on a millennial timescale. *The Holocene* **1**, 151–156.

Zhu, L., Zhen, X., Wang, J., Lü, H., Xie, M., Kitagawa, H., Possnert, G., 2009. A~ 30,000-year record of environmental changes inferred from Lake Chen Co, southern Tibet. *Journal of Paleolimnology* **42**, 343–358.

https://doi.org/10.1017/qua.2022.44 Published online by Cambridge University Press